

Article

Slatecalculation—A Practical Tool for Deriving Norm Minerals in the Lowest-Grade Metamorphic Pelites and Roof Slates

Hans Wolfgang Wagner ^{1,*}, Dieter Jung ², Jean-Frank Wagner ³ and Matthias Patrick Wagner ⁴

¹ Lehrstuhl für Geologie, Universität Trier, Im Nettetel 4, D 56727 Mayen, Germany

² Mineralogisch-Petrographisches Institut Universität Hamburg, Grindelallee 48, D 20146 Hamburg, Germany; Dieter.Jung@Jung1.de

³ Lehrstuhl für Geologie, Universität Trier, Behringstrasse 21, D 54296 Trier, Germany; wagnerf@uni-trier.de

⁴ Institute of Geography, Kiel University, D 24118 Kiel, Germany; m.p.wagner@gmx.de

* Correspondence: wagnerw@uni-trier.de

Received: 3 March 2020; Accepted: 26 April 2020; Published: 29 April 2020



Abstract: Roof and wall slates are fine-grained rocks with slaty cleavage, and it is often difficult to determine their mineral composition. A new norm mineral calculation called slatecalculation allows the determination of a virtual mineral composition based on full chemical analysis, including the amounts of carbon dioxide (CO₂), carbon (C), and sulfur (S). Derived norm minerals include feldspars, carbonates, micas, hydro-micas, chlorites, ore-minerals, and quartz. The mineral components of the slate are assessed with superior accuracy compared to the petrographic analysis based on the European Standard EN 12326. The inevitable methodical inaccuracies in the calculations are limited and transparent. In the present paper, slates, shales, and phyllites from worldwide occurrences were examined. This also gives an overview of the rocks used for discontinuous roofing and external cladding.

Keywords: mineralogy; roof slates; shales; phyllites; norm mineral calculation; hydro-micas; illite

1. Introduction

Under the term “roof and wall slates”, rocks that have good cleavage and high suitability for overlapping and discontinuous roofing as well as external cladding. Most of them are transversely schistose, very-low-grade metamorphic silt, and clay slates (more precise definitions in [1]). Occasionally, shales are included as well although they are stones that have no schistosity or slaty cleavage due to folding and orogenesis. Their good cleavability originates only from a fine sedimentary stratification (diagenetic foliation in the sense of [2]). Nevertheless, they are also used as roof and wall slates with a usual low thickness with an average of three or five millimeters [3].

Slate deposits are usually of a Proterozoic or Paleozoic age and usually originate from Caledonian and Variscan orogenesis. Unfolded parallel shales sometimes occur on old cratons (platforms). The fine grain size and the fine slaty cleavage, however, make it difficult to determine the composition quantitatively (e.g., polarization microscopy) [3]. Therefore, it can only be estimated by X-ray diffractometry (XRD).

Wagner et al. [4] tried to define very-low-grade metamorphic slates with the metamorphic phase diagram ACF/A'KF ($A = (Al_2O_3 + Fe_2O_3) - (Na_2O + K_2O)$, $A' = (Al_2O_3 + Fe_2O_3) - (Na_2O + K_2O + CaO)$, $K = K_2O$; $C \approx CaO$, $F = MgO + MnO + FeO$). However, this attempt did not go beyond a simple description. In a research project from 1989 to 1991, an attempt was made to use a full chemical analysis similar to the CIPW (Cross, Iddings, Pirsson, Washington; [5]) norm for magmatic rocks to make a rather inaccurate norm mineral evaluation for roof and wall slates ([6] and Table 2 therein).

Sericites (muscovite and paragonite), chlorite, quartz, and total carbonates were estimated as the main minerals. Ward and Gómez-Fernandez [7] used the Rietveld method-based Siroquant data processing system for X-ray powder diffraction analysis for the determination of the slate main minerals quartz, feldspar, micas, and chlorites. However, the application of the method was limited to low carbonate Spanish roofing slate. The determined feldspar (albite) values were higher than those of chlorite and are likely to be too high. Jung and Wagner [8] created a calculation method similar to the CIPW norm that was ready for practical use. They managed to determine the mineral constituents, and in particular, the content of free quartz with sufficient accuracy—for the first time—to some essential practical statements. The quartz content of a slate is, in addition to its structure and grain size, the most decisive factor for its workability (shape easily or heavily) [9,10]. It affects the brittleness and influences the edge straightness and flaking, punchability (making holes), smoothness and flatness of the cleavage surface, and thus, the cleavage thickness. In the slate industry, these characteristics affect the speed and profitability of production.

The petrographic description within EN 12326 [11] provides a rough estimation of the main and accessory constituents from thin sections and a measurement of minerals involved in mica layers and schistosity. Such estimated values are increasingly used to determine the quality and origin while ignoring inaccuracies, natural variations, and the limited sample of a thin section (first criticism in [3]). The norm mineral calculation presented here could replace this method. The results of such norm calculations have already been used not only in test certificates, but also in a manual [10]. Other authors cited such norm calculations together with results of other analyses and found good matches [9]. The results of more than 20 years of application of “slatenorm” [6,9,10,12–15] have shown that the inclusion of additional ore minerals, color-giving minerals, and hydro-micas (especially illite) in the new slate calculation is reasonable.

2. Materials and Methods

2.1. Colors

In addition to the normal black to bluish gray colors (generally short “black slate”), there are also so-called “color slates” with green and purple and/or red hues. It has been well known since [16] that the color of a slate depends on the $\text{Fe}^{2+}/\text{Fe}^{3+}$ -ratio. Therefore, FeO or Fe_2O_3 should be distinguished in wet-chemical roofing slate full analyses, as done in the extensive analyses by [6,16]. The entire data set of black, green, and red/purple slates and shales is shown in Figure 1. Black slate samples show Fe_2O_3 contents of 0% to 3%, green samples from 0.7% to 7.7% and red/purple samples from 4% to about 10%. The green color is caused by Fe-chlorite, and the red/purple colors by hematite. In the black color, however, the carbon content is more important [17]. This should also be reflected in the results of a norm mineral calculation.

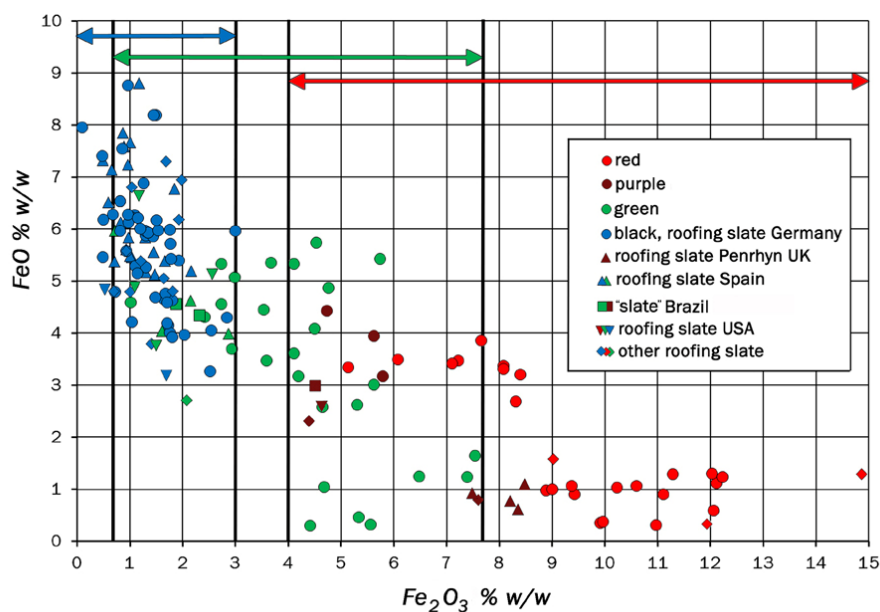


Figure 1. The dependency of slate color on the $\text{Fe}_2\text{O}_3/\text{FeO}$ ratio (analyses from [6,16,18–20] and own data).

2.2. Slate Samples

Based on experience, 363 chemical analyses of roofing slates from all over the world were subdivided into groups (Table 1) (e.g., [12,21]), using mostly average values, see Supplementary Materials: Tables S1a to 1h). From these, the standard norm minerals were determined with slatecalculation (Supplementary Materials: Tables S2a to 2h).

The “normal” slate originated from the Iberian—(59 samples) and Central Europe Variscides (69 samples). They are cleavable to usual thicknesses of 3 mm or 5 mm on average. In addition, they have good rock and selection quality, proven durability, and low oxidation susceptibility. The slates of the Iberian Variscides are very common in the world market. Central European as well as Iberian slates have been used for roofing since Roman times (see Figures 2–4).

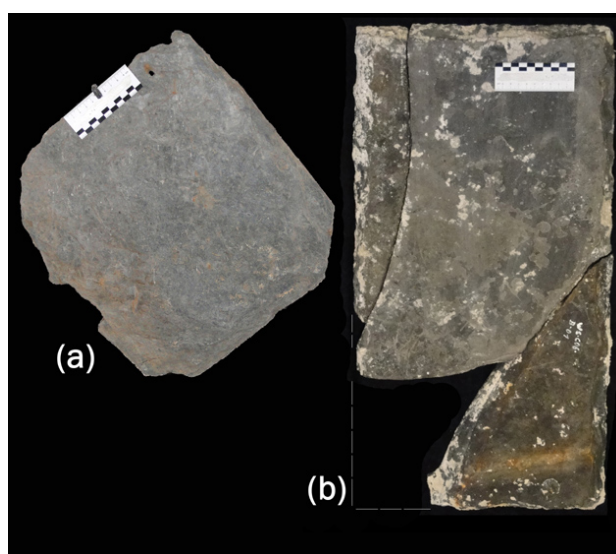


Figure 2. Roman slates: (a) Roman Slate, Central Europe; (b) Roman Slate, Liguria/Italy (based on [13]).



Figure 3. Underground slate mining in Spain (Valdeorras, Casaio-formation).



Figure 4. Opencast slate mining in Spain (Valdeorras, Luarca slate).

The type “carbonate slate” (21 samples) is defined in EN 12326 [11] as slates with at least 20% carbonate. They are the exception in the slate market and only of regional significance. The most well-known deposit of this type is in Liguria (Italy) and has been used locally for roofing slates in thicknesses of more than 6 mm since Roman times (Figure 2b; [13]). This slate changes its color from black to light grey at the latest after a few years on the roof. This characteristic is aesthetically favored in the region. The Ligurian slate has a good reputation even outside of the region and is used as freestone (natural stone) or for pool tables. The sample from Central Europe (Germany, Supplementary Materials: Tables S1c, S2c) comes from a now closed deposit. The slate example from China is still imported to UK but has some quality problems.

The 94 samples of the group “high carbon content” are slates with organic carbon content higher than 1.0%. EN 12326 [11] excludes roofing slates with carbon contents above 2% (Supplementary Materials: Tables S1d and S2d). This decision goes back to experiences in the well-known roofing slate deposits in Thuringia (Germany). Here high-quality roofing slates with normal C contents and a high lifetime on the roof were used (so-called “Blauer Stein”). In addition other varieties with darker colors and higher C contents have been used (so-called “Dunkler Stein” and “Dunkelkiesiger Stein”). The so-called “Rußschiefer” had the highest C content of more than 2% (from 3.3% to 4.9% after [22]) and a roof lifetime of only a few years. The other samples of this group come from the Himalayan and Southeast Asian Alpides. For samples from Bhutan, lifetimes beyond 70 years are declared [23]. The slate from Lai Chau (Vietnam) was lying on the roof of the opera-house of Hanoi for more than 50 years before it was renewed with the same slate.

Most (26 out of 29) samples of the group “with carbonate” originated from the Middle Devonian in the Central European Variscides (Supplementary Materials: Tables S1e and S2e). These always have carbonate contents above 5% and up to a maximum of 20%. They change in color from dark blue-grey to grey after approximately 10 years and can develop slightly reddish and brownish oxidation colors (Figure 5b,c). Their durability on the roof is sometimes lower than that of other “normal” slates from the Central European Variscides or “normal” slates from North-America or China (Figure 6).

Table 1. The geological information of the slate samples analyzed in this paper (also based on [4,6,9,12,14,15,18,24].

| Country | Province | Region/Location | Ø of Samples | Type of Rock | Formation | Series/System | |
|--|------------------------|---|--------------|----------------|--------------------------------------|---|------------------|
| “normal” slate, Iberian Varicides | | | | | | | |
| Spain | Asturia | Oscos | Vilarchao | 2 | Luarca | Middle Ordovician | |
| | | Alto Bierzo | Anllares | 2 | | | |
| | | | Mormeau | 8 | | | |
| | | | Los Molinos | 8 | | | |
| | Galicia/Orense | Valdeorras | | Riodolas | 5 | Argüeira | Upper Ordovician |
| | | | | Rozadais | 3 | | |
| | | | | Penedo Rayado | 6 | | |
| | | | | Los Campos | 2 | | |
| | Castile and León | La Cabrera | | San Pedro | 2 | Rozadais | |
| | | | | Benuza | 2 | | |
| | | | La Baña | 2 | | | |
| | | | San Vicente | 2 | | | |
| Spain | Galicia/Orense | Quiroga | | Pacios gris | Luarca | | |
| | | | | Pacios negra | | | 7 |
| | | | | La Campa negra | | | 1 |
| France | Anjou | Angers | Trélazé | 2 | Grand-Auverné (Trélazé Mb.) ≈ Luarca | | |
| Portugal | Porto | | Valongo | 1 | Valongo ≈ Luarca | | |
| | | | Arouca | 1 | | | |
| “normal” slate, Central European Varicides | | | | | | | |
| BeLux | Ardennes | | Martelange | 2 | Schiste ardoisier | | |
| | North Rhine-Westphalia | | Venn | 21 | Revin 4/5 | Black shales | |
| Germany | Rhineland-Palatinate | Eifel | | Katzenberg | Siegenian | Leutesdorf or Aubach | |
| | | | | Bausberg | | | 2 |
| | | | | Margaretha | | | 7 |
| Netherland | Xanten Nijmegen | from a Roman building from a Roman wreck | | | slate | | |
| | | | | | | | 2 |
| Germany | Rhineland-Palatinate | Hunsrück | | Moselberg | Lower Emsian | Hunsrück slates Altlay Hunsrück slates, Kaub | |
| | | | | Altlay | | | 1 |
| | | | | Bundenbach | | | 5 |
| Germany | Rhineland-Palatinate | Middle Rhine | | Kaub-Bacharach | Lower Emsian | Singhofen | |
| | | | | Singhofen | | | 1 |
| | Hesse | Lahn | | Langhecke | 1 | Adorf | Bänderschiefer |
| | | | | Lotharheil | 1 | | Bordenschiefer |
| Czech Rep. | Moravia | | Olomouc | 5 | Kulm | Moravice | |
| | | | | | | Mississippian Carboniferous | |

Table 1. Cont.

| Country | Province | Region/Location | | Ø of Samples | Type of Rock | Formation | Series/System | |
|-----------------------------|------------------------|-----------------------|-------------------|--------------|-----------------|-------------------------------------|---------------------------------------|--------------------------|
| carbonate slate | | | | | | | | |
| Germany | North Rhine-Westphalia | Nuttlar | | 1 | | Flinz | Middle to Upper Devonian | |
| Italy | | Liguria | | 3 | | Val Lavagna | Upper Cretaceous | |
| Switzerland | Glarus | Engi | Landesplattenberg | 1 | carbonate slate | Nordhelvetischer Flysch, Engi Slate | Eocene | |
| China | Hubei | Daba Shan | Pingli | 1 | | Pingli | Lower Ordovician | |
| Uruguay | Lavalleja | Arr. Minas Viejas | | 12 | | Minas Viejas group | Paleoproterozoic | |
| | | Arr. Mataojo | | 3 | | Mataojo group | | |
| high carbon content | | | | | | | | |
| | | Eifel-Venn | Elise | 7 | | Salm 1/2 Tremadoc | Lower Ordovician | |
| Germany | North Rhine-Westphalia | | | 1 | | Hangenberg | Upper Devonian to Lower Carboniferous | |
| | | Marsberg | | 24 | | | Lydit | Lower Carboniferous |
| | | | | 10 | slate | Kulm | Posidonia Clayshales (Marsfeld?) | |
| | | | | 15 | | | Lower Alum | |
| | | | | 28 | | | | |
| Thuringia | Ronneburg | | 3 | | Leder Slate | Upper Ordovician to Lower Silurian | | |
| | | Lehesten Schmiedebach | | 3 | | Kulm Lehesten dunkelkiesig | Mississippian Carboniferous | |
| Bhutan | | Wangdu Phodrang | | 2 | | above the Chekha | Triassic? | |
| Vietnam | Lai Chau/Dien Bien | Quang Chêng | | 1 | | schiste ardoisier | Triassic | |
| slate with carbonate | | | | | | | | |
| Germany | Hesse | Lahn-Dill | Haiger | 2 | | | | |
| | | | Batzbach | 1 | | | Wissenbach | |
| | Rhineland-Palatinate | Lahn | Rupbach | 2 | | Eifelian | Middle Devonian | |
| | North Rhine-Westphalia | Bad Fredeburg | Magog | 12 | slate | | | Fredeburg (≈ Wissenbach) |
| | | | Felicitas | 7 | | | Wissenbach) | |
| | Hessen | Willingen | Brilon | 2 | | Asten (≈ Wissenbach) | | |
| Switzerland | St Gallen | Calanda | Pfäfers-Vadura | 1 | | Kalkthonschiefer | Eocene | |
| U. S. A. | New York | | Red | 1 | | Poultney | Cambrian to Ordovician | |
| | Pennsylvania | | Lehigh | 1 | | Martinsburg | Middle to Upper Ordovician | |

Table 1. Cont.

| Country | Province | Region/Location | Ø of Samples | Type of Rock | Formation | Series/System | | |
|---|--------------------|--------------------------------------|-------------------|--------------|---------------------|---------------------------------------|------------------|---------------------|
| Other slate UK, N-America, China | | | | | | | | |
| UK | Wales | Penrhyn | purple | 5 | Llanberis | Cambrian | | |
| Canada | Newfoundland | Trinity Bay | purple green | 3 1 | Bonavista | | | |
| U. S. A. | Vermont | variegated | Sea green | 1 | Poultney | Cambrian to Ordovician | | |
| | | | Unfading green | 1 | | | | |
| | New York | Eureka | 1 | slate | Trenton Poultney | | | |
| China | Hubei Shaanxi | Hongshigou Ziyang | purple black | 1 1 | Daguiping | Lower Silurian | | |
| | | | Bright green | 1 | | | | |
| | | | | 3 | s 1ds | | | |
| | | | | 2 | | | | |
| shales | | | | | | | | |
| Botswana | Southern District | Kanye | | 1 | Platberg Group | Rietgat | Neoproterozoic | |
| Nigeria | Ebonye | Southern Benue trough | | 3 | Asu River Group | Abakaliki | Lower Cretaceous | |
| Brazil | Minas Gerais | Papagaios, Paraopeba, Sete Lagoas | black | 1 | shale | Bambui, Santa Helena | Neoproterozoic | |
| | | | oliv green | 2 | | | | |
| | Santa Catarina | | purple | 1 | Tubarao | Mafra | Permian | |
| | | | dark green, black | 1 | | | | |
| | | | | 2 | | | | |
| Germany | Baden-Wuerttemberg | Dotternhausen | Tafelfleins | 1 | carbonate shale | Posidonia | Lias ε | Lower Jurassic |
| Norway | Finnmark | Vestertana | red | 1 | shale | Finnmark Supergroup | Vestertana Group | Riphaen Proterozoic |
| | | | green | 1 | | | | |
| Switzerland | Zurich | Weiach | | 4 | shale (high carbon) | Lower Rotliegendes, lakustrine series | Permian | |
| | | | | 1 | | | | Carbonate shale |

Table 1. Cont.

| Country | Province | Region/Location | Ø of Samples | Type of Rock | Formation | Series/System | |
|-----------------------|-----------------------------|-----------------|------------------|--------------|------------|---------------------------------|--|
| schists and phyllites | | | | | | | |
| Spain | Castile and León | Segovia | Bernardos | 4 | phyllite | Schists-Metagraywacke Complex | Neoproterozoic to Lower Cambrian |
| | Galicia | A Terra Cha | Verde Lugo | 2 | | Cándana Group | Lower Cambrian |
| Portugal | Trás-os-Montes e Alto Douro | | Foz Coa | 1 | Quar-tzite | Desejosa | Lower Cambrian |
| Norway | Finnmark | | Alta | 1 | | Alta Group | Riphaen Proterozoic |
| Belgium | Wallonia | Ardennes | Friarfjord | 2 | phyllite | Laksefjord group | Early to Middle Ordovician |
| | | | Vielsalm | 1 | | Salm Group | |
| Germany | Saxony | Vogtland | Ottre redschist | 8 | phyllite | Phycodendachschiefer | Lower Ordovician |
| | | | Ottre coticule | 25 | | | |
| Czech Rep. | | | Theuma, Oelsnitz | 1 | phyllite | Kralupy-Zbraslav group | Proterozoic Cambrian to Ordovician |
| | | | Rapštejn | 2 | | | |
| India | Himachal Pradesh | | Zelezny Brod | 1 | phyllite | Radčice Group | Proterozoic Neo- to Mesoproterozoic Ordovician |
| | | | Himachal | 1 | | Chamba and Katarigali | |
| Argentina | Cuyo | | Bectel | 1 | phyllite | Delhi Supergroup Ajabgarh Group | Mesoproterozoic Ordovician |
| | | | San Luis | 2 | | San Luis | |

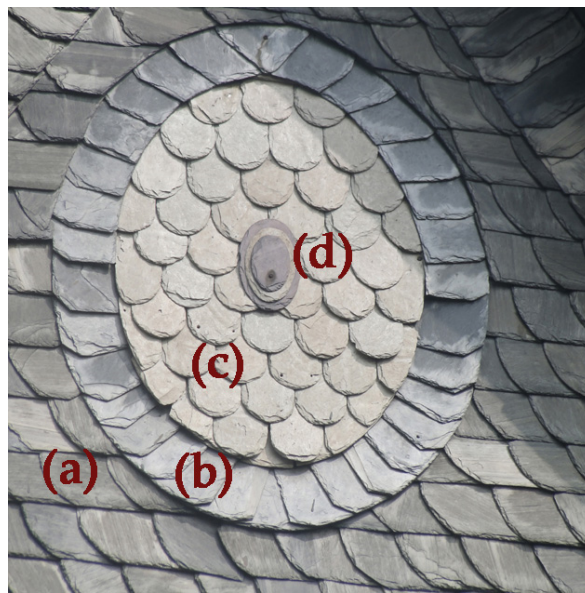


Figure 5. The partly filigree slate coverings of ornaments with round forms in Central Europe require well workable slates; four different deposits and varieties: (a) black, hard, Upper Devonian; (b) black, with carbonate, Middle Devonian; (c) green, with carbonate, Middle Devonian; (d) purple, hard Lower Devonian; (slate covering at least 90 years old).



Figure 6. The imported slates (China and Canada) on the Saint Nicolai Church in Plön, arranged in “English” rectangle roofing with hooks (15 years old).

Rocks of the group “Shales” (19 samples) lack schistosity (tectonic or slaty cleavage) (Supplementary Materials: Tables S1h, S2h). Their cleavage results only from a fine sedimentary stratification (Figure 7). All samples with this structure have inferior workability, especially punchability, compared to normal roofing slates. The most economically important “shale” deposits worldwide are located in the Neoproterozoic Bambui formation in Brazil [19]. This is the most important source for slates used for flooring and facades in the world. Roofing slate is a by-product and is exported mainly to countries using predominantly rectangle slates, including the USA and UK. The “shales” from the Neoproterozoic of South Africa are also of transregional importance. All other samples, like the ones from Central Europe, have or had only local importance. An example for this is the “Tafelfleins”. This is a layer in the Lias ϵ in the Lower Jurassic, which was once used as roofing slate, but fails to meet today’s requirements.

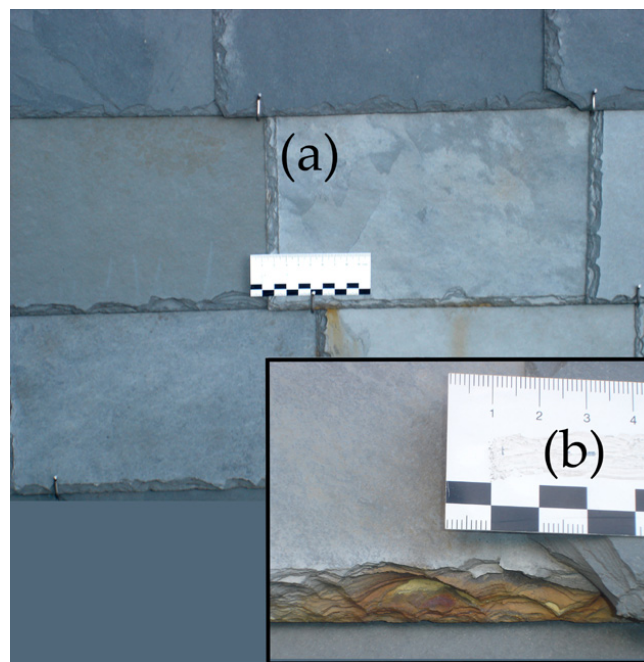


Figure 7. The cleavage of the shale does not originate from real schistosity but from a fine stratification (a). (See picture detail on the lower right (b)) (At the time of the photo a nearly new cladding.); Minas Gerais (oliv-grey)/Brazil.

The 52 samples of the group “schists and phyllites” are slates of a higher metamorphic state (“low-grade metamorphism” instead of “very-low-grade metamorphism”, see Figure 8) (Supplementary Materials: Tables S1g and S2g). In the classical slate areas of Central and Western Europe, their use is rare, or they are only used in ornamental covers solely because of their color (e.g., green). Nevertheless, they are typical for some mountainous regions in the Alps or Scandinavia.



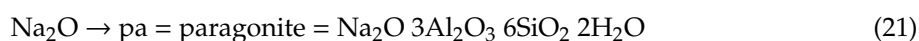
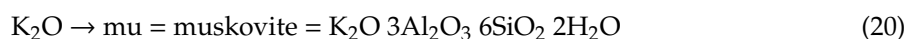
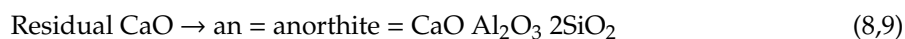
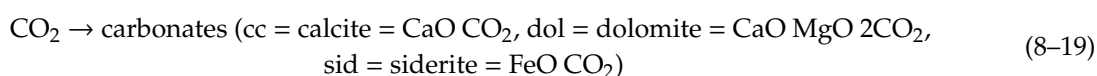
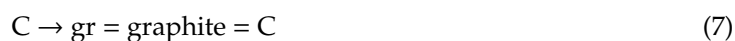
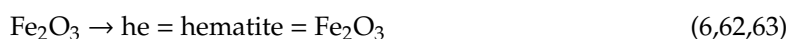
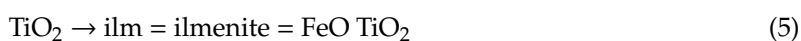
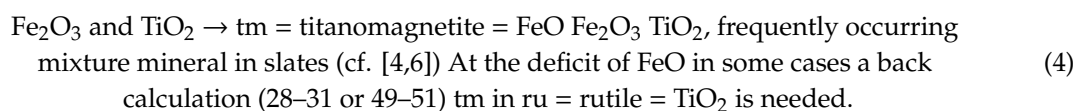
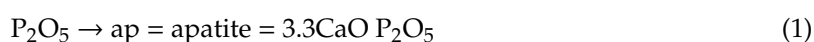
Figure 8. Phyllitic Quartzite facade panels (transverse length = 50 cm) (almost 60 years old); Alta Quartzite/Norway.

2.3. Algorithm Slatecalculation

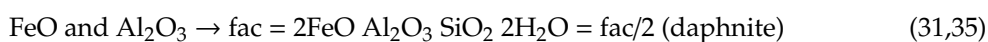
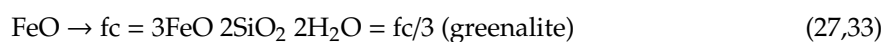
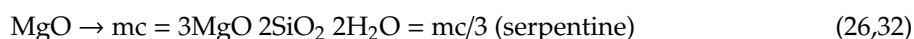
The extended method slatecalculation presented here is based on a previous, unpublished program called “slatenorm” [8,25] (see Supplementary Materials).

In a first step, the extended algorithm includes the distinction of sulfides. So far, pyrite was the only sulfide calculated in “slatenorm”. This is inaccurate, as pyrite prevails only in less metamorphic slates (like in the Ardennes or Rhenohercynian Zone, Supplementary Materials: Tables S1b and S2b). In many higher metamorphic slates (e.g., from Spain) phyrrotite is predominant and should be included in the calculation because it is more susceptible to oxidation. Therefore, in a first step, the extended algorithm differentiates various sulfides.

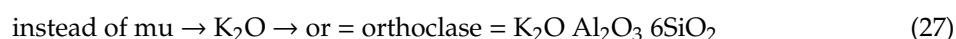
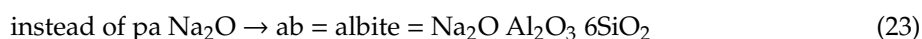
The basic calculations of the algorithm, fundamental norm minerals, and chemical formulas are described in a very simplified form below. The detailed calculations can be found in the Supplementary Materials: a flow chart of procedures as well as the computing program in a screenshot of the Excel program “slatecalculation”, and they are numbered as follows:



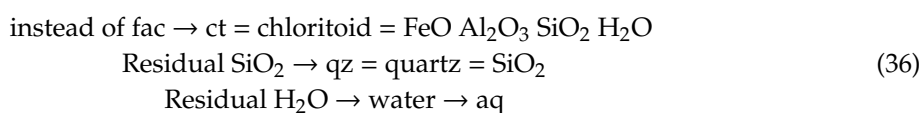
The very variable minerals of the chlorite group require more complicated considerations with regard to their composition:



With the negative rest of $\text{Al}_2\text{O}_3 \rightarrow (\text{ab, or}) = \text{feldspars}$:



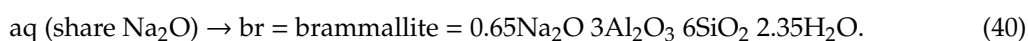
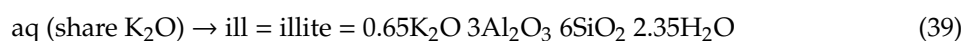
In case of high Al_2O_3 – contents the calculation of chloritoid might be necessary:



The remaining $H_2O = aq$ may have a positive or negative value, and this is the basis for an extended algorithm determining hydro-micas. In the input data, carbon compounds (e.g., CO_2 and organic C) and elementary Sulphur (S) are not included in the glow loss (or loss of ignition (LOI)), but rather subtracted. Furthermore, in the case of predominant FeO compounds, the description of the total amount of Fe as Fe_2O_3 leads to an unrealistic oxidation gain at the expense of the LOI. Only a carefully corrected LOI can be incorporated in the norm calculation as $H_2O = aq$ but will still be less precise. Thus, the calculated data will have a higher range of variation.

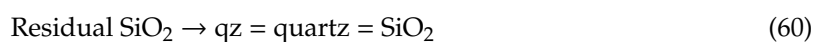
2.4. Hydro-Micas

A positive aq value is the basis for the hydro-micas calculation (see Supplementary Materials: flow chart, steps of calculation 40 to 60). The original values, as well as the results of calculation steps 9 (Al_2O_3 and SiO_2) and 17 or 19 (MgO and FeO) are used as the starting point.

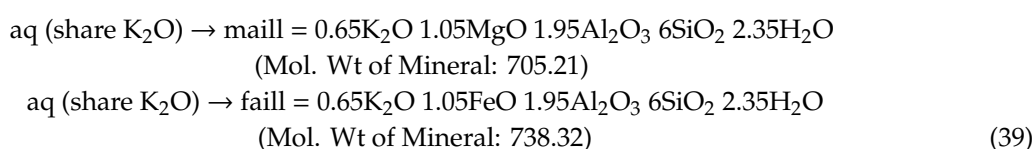


The calculation of hydro-micas requires a recalculation of the remaining phyllosilicates, like micas (mu, pa, steps 41 and 42) and chlorites (mac, mc, fac, fc, steps 47 to 59).

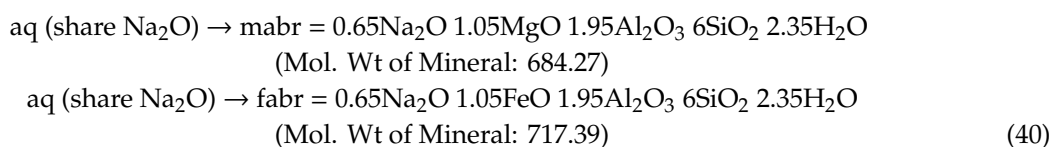
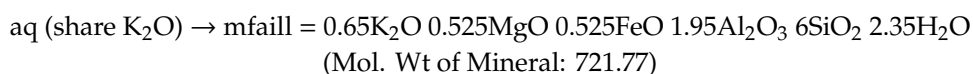
If aq —contents > 0 , the calculation of limonite is necessary as well:



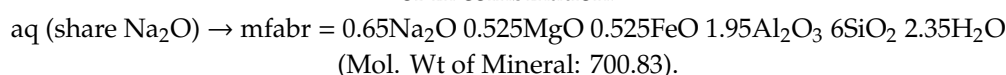
If the ill and br values are exceptionally high, in rare cases, MgO and FeO can remain after the calculation and lead to an Al_2O_3 -deficit. In this case, the following varieties may be calculated as hydro-micas:



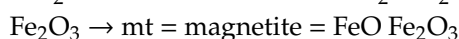
or in combination:



or in combination:



If the first calculation steps yield negative values or additional information about other minerals is available, further calculations may be considered (e.g., Alta-Quartzite-schist and others):



$\text{MnO} \rightarrow \text{sp} = \text{spessartine} = 3\text{MnO Al}_2\text{O}_3 3\text{SiO}_2$.

As a final step the norm minerals are added up to minerals and/or mineral groups:

- | | |
|--|-----|
| an + ab + or = feldspars | (a) |
| cc + dol + sid = carbonates | (b) |
| mu + pa = micas | (b) |
| ill + br = hydro-micas | (d) |
| mac + fac + mc + fc = chlorites | (e) |
| pn + pt = sulfides | (f) |
| pn + pt + tm + ilm + ru + he (+ mt) = ore-minerals | (g) |
| qz + an + ab + or (+ sp) = rigid minerals | (h) |
| mu + pa + ill + br + mc + mac + fc + fac = elastic minerals. | (i) |

2.5. Analysis of the Fabric of Phyllosilicates

The petrographic analysis in EN 12326 [11] can be used to estimate the structure of the slate. An important measurement is the mica layers count (better: phyllosilicate layers) per mm in thin sections. This indicates the possible splitting thickness of the slate. Furthermore, the perfection of the phyllosilicates fabric (often simply called the mica fabric) is important for the weathering resistance (perfection in terms of EN 12326-2 [11]: “phyllosilicates are continuous and tied together they will form a net”). In simple terms, the phyllosilicates, with a perfect net structure enclose the weatherable minerals, and protect them against weathering [4,6].

3. Results and Discussion

The mineral contents computed by slatecalculation show proper values for the different slate varieties: The Roman slate shown in Figure 2a is a normal slate from the Lower Devonian, for which slatecalculation calculates the normal mineral quartz 30.0 +/- 4.4%, micas 41.3 +/- 2.5%, hydro-micas 5.5 +/- 4.2%, chlorites 16.8% +/- 2.9 and carbonates 1.6 +/- 0.5. Roman Slate, Liguria/Italy (Figure 2b) is a carbonate slate with quartz 18.3 +/- 1.8%, micas 19.0 +/- 1.7%, hydro-micas 4.0 +/- 3.8%, chlorites 5.4 +/- 0.6% and carbonates 50.2 +/- 4.3% (based on [13]). The 21 roof slate samples from the Casaio formation (Upper Ordovician, Figure 3) in Valdeorras are normal low-carbonate slate with an average mineral content of quartz 31.3%, micas 51.1%, hydro-micas 0.1%, chlorites 12.6%, carbonates 0.2%, sulfides 0.2%, and phyrrotite 0.1%. The sample from the Luarca formation (Valdeorras, Figure 4, Middle Ordovician.) shows quartz 28.6%, micas 40.3%, carbonates 0.4%, sulfides 1%, and a higher phyrrotite content of 0.6%. The partly filigree slate coverings of ornaments (Figure 5) require well workable slates. Norm minerals of three different varieties are (slatecalculation): Black, hard (Figure 5a: quartz 53.0%, micas 21.8%, hydro-micas 8.2%, Fe-chlorites 7.0%, Mg-chlorites 4.0%, carbonates 2.0%; black, with carbonate (Figure 5b): quartz 25.3%, micas 16.0%, hydro-micas 17.7%, Fe-chlorites 5.91%, Mg-chlorites 10.3%, carbonates 12.4%; green, with carbonate (Figure 5c): quartz 27.2%, micas 35.0%, hydro-micas 2.9%, Fe-chlorites 6.7%, Mg-chlorites 6.9%, carbonates 11.0%. The two import slates from the church in Plön (Figure 6) come from overseas: Ziyang/China (black) quartz 45.4%, micas 25.5%, hydro-micas 2.2%, carbonates 0.8%; Trinity Bay/Canada (purple) quartz 30.5%, micas 42.0%, h-micas 2.8%, carbonates 0.4%. The following norm minerals were calculated for the shale from Minas Gerais (oliv-grey, Figure 7): quartz 33.1%, feldspars 14.4%, micas 31.5%, hydro-micas 1.8%, carbonates 1.8%, sulfides 0.3%. The calculated norm minerals of Alta Quartzite (Figure 8) are quartz 57.9%, feldspars 25.4%, micas 7.8% and carbonates 3.0%. All results of the norm minerals calculated by slatecalculation

are petrographically coherent, rational, and free of contradictions (for example, normally no negative results for norm minerals) (Supplementary Materials: Tables S2a to S2h).

The differences between the results of slate calculation compared to the previous version slatenorm can be seen when comparing the results of the main minerals quartz, mica, chlorite, carbonate, and feldspar in Figure 9. The differences between slatenorm (blue) and slate calculation (red) are not significant (Figure 9). There are only significant differences if hydro-micas are calculated. In the case of slate calculation, only a carefully determined LOI can be incorporated in the norm calculation of hydro-micas (slate calculation). It will still be less precise and show a larger range of variation. The slates of the Iberian Variscides have only a low content of hydro-micas (0% to 7%), so there are only slight differences in the two methods (Figure 9). The differences are higher in the case of the samples of the Central European Variscides with hydro-micas contents of 5% to 24%. As more Al_2O_3 is used in the calculation of hydro-micas in slate calculation, the calculation in a few cases results in higher contents of feldspars (ab and or; steps 44 and 46 in the algorithm, Section 2.3) than in the previous calculation slatenorm (see steps 23 and 25 in the algorithm, Section 2.2) (Figure 9c). The slightly lower chlorite content in the slate calculation compared to slatenorm is due to the calculation of the norm mineral titanomagnetite (tm) instead of ilmenite (ilm) or rutile (ru) (Figure 9a). The differences between the results of the two methods lie in the range expected by the authors.

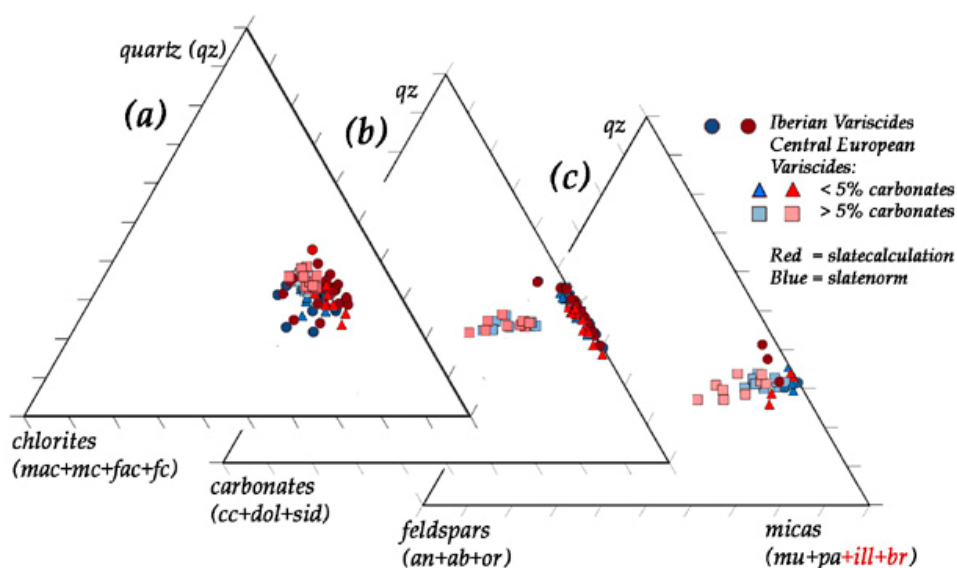


Figure 9. Comparison of the main minerals calculated with slatenorm (blue) and slate calculation (red). (a) quartz/micas/chlorites, (b) quartz/micas/carbonates, (c) quartz/micas/feldspars.

Table 2 shows a rough overview of the practical roofing slate characteristics and which minerals influence them [3,4,6,9,12,14,21,26]. The classification “positive” or “negative” can only be considered as a rough indication for slate quality. Different uses usually also require different assignments. The hardness of the slate, higher quartz content, and the associated higher bending strength are considered positive in UK as they allow the production of larger rectangular formats and the use in areas of high wind load. In contrast, this is different when round and even filigree shapes are desired, as a higher quartz content makes such a processing more difficult (e.g., in Germany, Figure 5b,c).

Moreover, weathering colors can be desirable in the conservation of monuments and historic buildings. Such colors in combination with carbonate percentages above 3% unfortunately bring a shorter lifetime for the roof. The quality of slate is not only determined by the mineral content, but also the fabric of micas (better: fabric on phyllosilicates) (schistosity and, slaty cleavage), which essentially determines the gap cleavability [3,4,6,9,11,12].

Table 2. Minerals and their influence on practical roofing slate quality.

| Norm Minerals | | | Positive | | Negative | Color | | |
|---------------|--|------------------------|-------------------------|--|---------------------------------|--|--|--|
| | Quartz | qz | | mechanical strength, hardness | resistance to weathering | > 32% w/w brittleness, sometimes worse cleavability, punching quality and finishing quality in round forms | | |
| feldspars | Orthoclase Albite Anorthite | or ab an | Ridged minerals | (have a cleavability) | | | | |
| micas | Muscovite Paragonite | mu pa | | cause the cleavability, punching quality and finishing quality also in round forms | resistance to weathering | | | |
| hydro-micas | Illite Brammalite | ill br | Elastic minerals | help with cleavability, punching quality and finishing quality | | product of weathering | | |
| chlorites | Mg-Al-Chlorite Mg-Chlorite Fe-Al-Chlorite Fe-Chlorite | mac mc fac fc | | | | | blue, green | |
| carbonates | Calcite Dolomite Siderite | cc dol sid | | (have a cleavability) | | > 5% w/w after EN 12326-1 thickness increase | with higher contents > 5% w/w less resistant to weathering > 0.3% w/w and in accumulations oxidation risks | light grey with oxidation colors weathering ("semiweathering") |
| ore minerals | Pyrrhotite Pyrite | pn pt | | | | | in accumulations of micro pyrites oxidation risks | |
| | Hematite Limonite | he lm | | | | | product of weathering | > 2% w/w red, purple |
| | Graphite | gr | | | | 2% w/w after EN 12326-1 does not permit | | black |

The shales without schistosity have only a fine stratification and no phyllosilicate net structure. As a result, they have no protective effect. If harmful components, such as sulfides are embedded in these fine layers of stratification, oxidation occurs (Figure 7).

The phyllosilicates calculated in slatecalculation show a total mica content from usually above 40% (up to a maximum of 60%) and a chlorite content from more than 10% (up to a maximum of 25%) in normal slates (Figure 10a). Only for samples with higher carbonate (“carbonate” and “with carbonate”) or higher carbon (“high carbon content”), are the proportions lower. The micas (mu+pa+ill+br) predominate over the chlorites (mac + mc + fac + fc) in a ratio of 3 to 1.

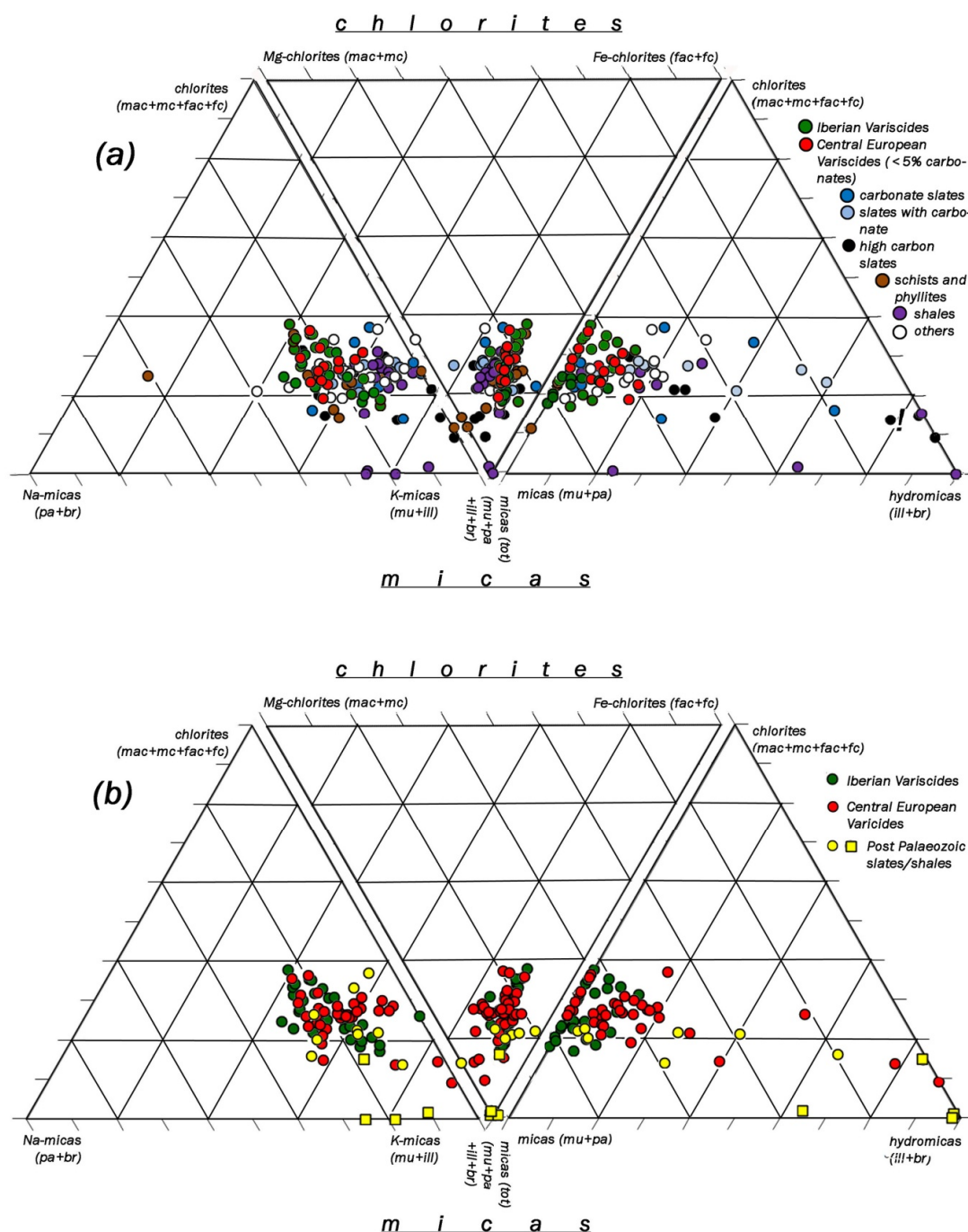


Figure 10. Phyllosilicates as calculated by slatecalculation (a) Types of phyllosilicates; (b) selection of different deposits.

In “normal” slates, the Fe-chlorites content (fac + fc) outweighs the Mg-chlorites content (mac + mc).

The calculated proportion of hydro-micas (ill and br) could reflect (in addition to the Kübler Index or the organic matter reflectance [26,27]) the degree of metamorphism in most of the samples. That is why phyllites always have hydro-mica values of 0% in the calculation outputs.

The slates of the Iberian Variscides also show very low positive percentages of hydro-micas, while slates from the Central European Variscides (Ardennes and Rhenohercynian zone) have a lower metamorphic grade and show higher values of hydro-micas (Supplementary Materials: Tables S2a and S2b).

Some Mesozoic and Cenozoic examples of “shales” and “carbonate” slates have higher values, up to a prevalence of hydro-micas. There may be other phyllosilicates (perhaps with swelling capacity) that are not calculated in the context of slatecalculation (Figure 10b). There are also exceptions, e.g., when hydro-micas appear as new minerals due the weathering of metamorphic rocks. The Ordovician-Silurian Lederschiefer from Thuringia is deeply weathered because of unstable mineral constituents (hence the name), which can be seen by a high content of hydro-micas (see “!” in Figure 10a). The K-micas (mu + ill) are clearly more frequent than the Na-micas (pa + br).

There is a connection between the calculated “elastic” minerals and the mica-layers per mm in the sense of EN 12326-2 [11], which can be used for practical questions, such as possible thickness and cleavability. This relationship applies to “hard” slates only if the lengthening and orientation of the quartz is relevant as well (Figure 11).

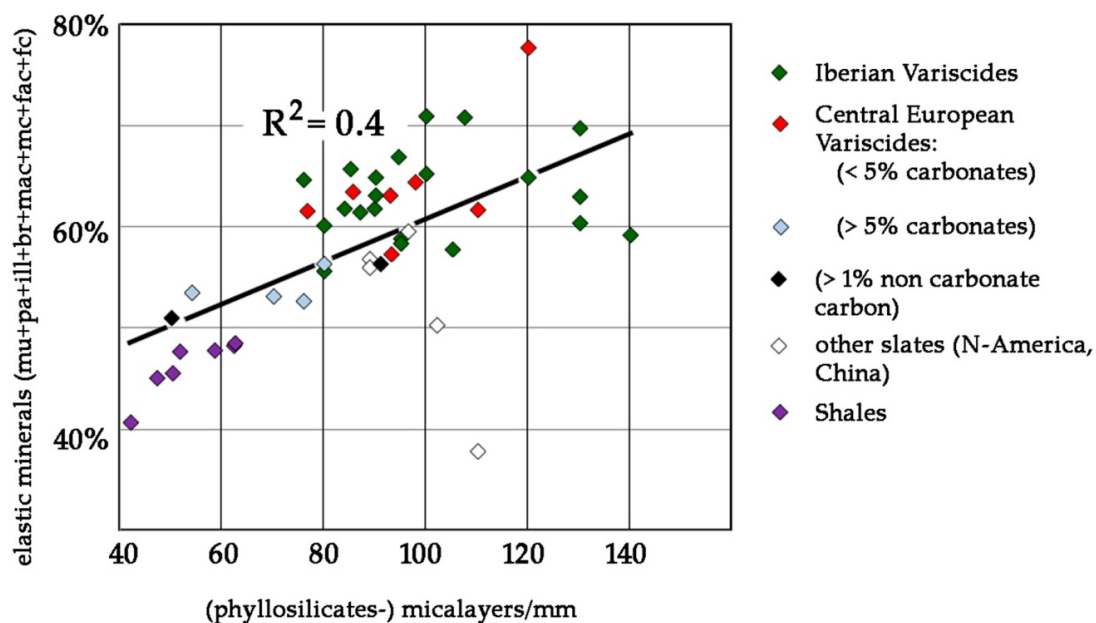


Figure 11. The relationship between calculated “elastic minerals” (see Table 2 and Section 2.4(i)) (slatecalculation) and the mica-layers per mm in the sense of EN 12326-2 [11].

There is a connection between the calculated “elastic” minerals and the mica-layers per mm in the sense of EN 12326-2 [11], which can be used for practical questions, such as possible thickness and cleavability. This relationship applies to “hard” slates only if the lengthening and orientation of the quartz is relevant as well (Figure 11).

When assessing the weathering resistance of slates on the roof, the location and orientation of the roof are important as well. Wagner [14] investigated military barracks in Germany that provided an ideal example for such weathering studies: Two different roofing slate types were studied on 29 similar buildings, all of similar age and exposed to similar weathering conditions.

The slates with carbonate (Central European Variscides) were considered to be less stable. This became clear from both the state of weathering and the water absorption of slates on the barrack roofs. For the “normal” slates (with less carbonates) (also from the Central European Variscides), the values are significantly better. The main wind and rain direction at the location is North–West.

When old roofs are examined in relation to their orientation to the main wind and rain direction side, the saying goes, “Roofing slate loves rain”. Since the different roofs of the barracks were built in different directions, it was possible to check this assumption. Roofing slates on the windward side were allegedly more stable than on the lee side.

The considerably better condition of roofs oriented to the windward side and covered with slates with carbonate confirmed the statement. Results for roofs covered with “normal” slates are similar but less distinct (Figure 12).

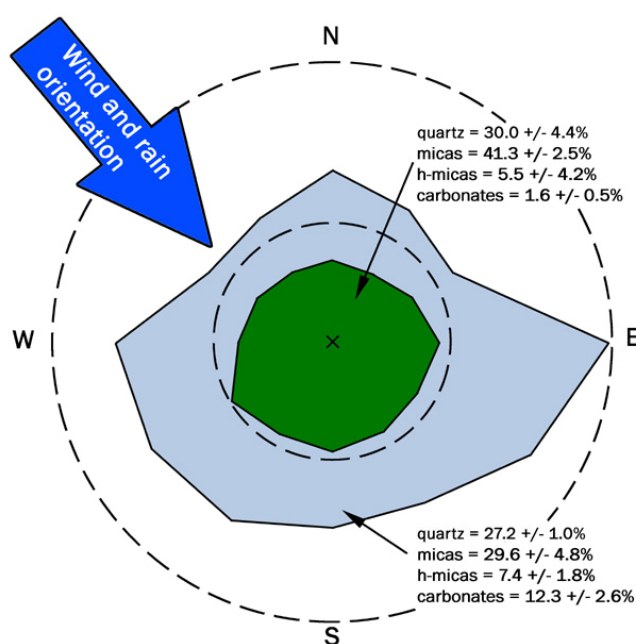


Figure 12. The dependence of weathering to the main wind and rain direction of slates “with carbonate” (turn blue) and “normal” slates (green): average values with inclusive standard deviation of some norm minerals. The distance from the center to the outside is the relative weathering intensity (altered based on [14]).

The norm mineral calculation slatecalculation (like its unpublished predecessor versions) has been developed to investigate important practical characteristics of roofing slate deposits and their products. Minerals that affect the durability or workability can be determined with this tool with sufficient accuracy. The result analysis is partly better than in the petrographic analysis of EN 12326 [11].

The open access publication of the algorithm online may encourage colleagues to test the method for other fields such as diagenesis, grade of metamorphosis, and provenance analysis, or for other fine-grained sediments and metamorphic rocks. The authors are very open to constructive criticism, improvements, and further experiences or results for further developments and improvements.

4. Conclusions

With the slatecalculation method for calculating norm minerals presented here, we introduced another method for determining the mineral content of lowest-grade metamorphic pelites and roof slates.

The calculated norm minerals are:

carbonates (cc = calcite, dol = dolomite, sid = siderite),
 feldspars (an = anorthite, ab = albite, or = orthoclase),
 micas (mu = muscovite, pa = paragonite),
 hydro-micas (ill = illite, br = brammallite),
 chlorites (mac+mc = Mg-chlorites, fac+fc = Fe-chlorites)
 sulfides (pt = pyrite, pn = pyrrhotite),
 other ore-minerals (tm = titanomagnetite, ilm = ilmenite, ru = rutile, he = hematite, lm = Limonit),
 others (ap = apatite, gr = graphite, ct = chloritoid),
 and qz = quartz.

With the norm mineral computation, this becomes a better, more exact and more easily reproducible tool. The inaccuracies of this method remain limited and transparent. The results are also comparable and sometimes more precise than other methods, such as X-ray diffraction (XRD) (Supplementary Materials: Table S3). It is also a good complement to microscopic thin section analysis, which is usually difficult due to the fine grain of the slate.

The different varieties of slate, such as normal slate, slate with carbonate, carbonate slate, high carbon slate, or quartz-rich slate can be accurately and precisely determined using slatecalculation. Slatecalculation can also help with this to estimate the practical raw material qualities of roof and wall slates (see Table 2). The elastic mineral contents calculated using this method also allows conclusions to be drawn about the microscopic structure of the slate (Figure 11, Supplementary Materials: Table S4). In contrast to thin-section microscopy, slatecalculation can be used to distinguish between micas (muscovite and paragonite) and hydro-micas (illite and brammallite). The method could also provide information (in addition to the Kübler Index or the organic matter reflectance [26,27]) about the degree of metamorphism with the calculated hydro-mica (e.g., illite-) content.

Supplementary Materials: The following are available online at <http://www.mdpi.com/2075-163X/10/5/395/s1>. Flow chart of procedures in “slatecalculation”; a, b, c, ... = conditions in the Excel program; 1, 2, 3, ... = calculation steps in the program. Screenshot of the Excel program slatecalculation. Tables S1a to S1h, chemical full analysis, (taken from [6,9,12,13,15,18,20,22,23] with added information and own analyses), Italic s = estimated values; Ø 5 = average of five single analyses. Tables S2a to S2h, results of slatecalculation norm calculations. Table S3, Comparison of XRD data and slatecalculation. Table S4, Mica-layers per mm and elastic minerals in % (slatecalculation). slateNorm.exe (use only “Grundversion!”). slatecalculation.xls can be requested by email: svschiefer@yahoo.de. References [28–30] are cited in the supplementary materials.

Author Contributions: Conceptualization, H.W.W.; methodology, H.W.W. and D.J.; software, H.W.W.; validation, H.W.W.; formal analysis, H.W.W.; investigation, H.W.W.; resources, H.W.W.; data curation, H.W.W.; writing—original draft preparation, H.W.W.; writing—review and editing, M.P.W. and J-F.W.; visualization, H.W.W.; supervision, J.-F.W. and D.J. All authors have read and agreed to the published version of the manuscript.

Funding: The publication was funded by Open Access Fund of Universität Trier and the German Research Foundation (DFG) within the Open Access Publishing funding programme. The development of the computer program “slatenorm” was funded by Rathscheck Schiefer und Dach-Systeme—ZN der Wilh. Werhahn KG Neuss, D 56727 Mayen-Katzenberg. The publication here was permitted.

Conflicts of Interest: The authors declare no conflicts of interest.

References

1. Arkai, P.; Sassi, F.; Desmons, J. Very low- to low-grade Metamorphic rocks. *Recomm. IUGS Subcomm. Syst. Metamorph. Rocks* **2003**, *5*, 1–12.
2. Passchier, C.W.; Trow, R.A.J. *Microtectonics*, 2nd ed.; Springer: Heidelberg, Germany, 2005.
3. Wagner, H.W. The basics of test methods of slates for roofing and cladding. Grundlagen für die Prüfung von Dach- und Wandschiefern. *Z. Dtsch. Ges. Geowiss.* **2007**, *158*, 785–805.
4. Wagner, H.W.; Le Bail, R.; Hacı, M.; Stanek, S. European roofing slates part 1: Remarks to the geology of mineral deposits. *Z. Angew. Geol.* **1994**, *40*, 68–74.

5. Winter, J.D. (n. s.). CIPW Norm Excel Spreadsheet. Available online: <http://webspaces.pugetsound.edu/facultypages/jtepper/MIN-PET/Norm%20Calculation.XLS> (accessed on 21 February 2020).
6. Wagner, H.W.; Baumann, H.; Negendank, J.; Roschig, F. Geological, petrographic, geochemical and petrophysical investigations on roofing slates. *Mainz. Geowiss. Mitt.* **1997**, *26*, 131–184. Available online: https://www.uni-trier.de/fileadmin/fb6/prof/GEO/baumann/pdf_files/slate.pdf (accessed on 21 February 2020).
7. Ward, C.; Gómez-Fernandez, F. Quantitative mineralogical analysis of Spanish roofing slates using the Rietveld method and X-ray powder diffraction data. *Eur. J. Mineral.* **2003**, *15*, 1051–1062. [[CrossRef](#)]
8. Jung, D.; Wagner, H.W. SlateNorm: Calculation of a normative mineral content of slates. Unpublished. 1998–2000.
9. Cárdenes, V.; Rubio-Ordóñez, A.; Wichert, J.; Cnudde, J.P.; Cnudde, V. Petrography of roofing slates. *Earth Sci. Rev.* **2014**, *138*, 435–453. [[CrossRef](#)]
10. Lorenz, W.; Gwodszy, W. Chapter 3.2 Roofing slate. In *Manual on the Geological-technical Assessment of Mineral Construction Materials*; Geol. Jahrbuch, Sonderhefte Reihe H, Heft SH 15; BGR: Hannover, Germany, 2003; pp. 276–290.
11. European Committee for Standardization (CEN). *EN 12326-1 and -2 Slate and Stone Products for Discontinuous Roofing and Cladding—Part 1: Product Specification 2014, Part 2: Methods of Test 2010*; Beuth: Berlin, Germany, 2010.
12. Jung, D. Zur Frage der Qualitätsbeurteilung von Schiefer. *Schr. Schiefer Fachverb. Dtschl. E. V.* **2009**, *10*, 75–107.
13. Wagner, H.W.; Schultheis, W. Römischer Dachschiefer—Neue Funde und neue Erkenntnisse. *Anschnitt* **2011**, *63*, 202–206.
14. Wagner, H.W. Geologische Untersuchung und Materialprüfung an Dachschiefer-Altdeckungen. *Mainz. Geowiss. Mitt.* **2014**, *42*, 121–142.
15. Morales-Demarco, M.; Oyhantçabal, P.; Stein, K.-J.; Siegesmund, S. Dolomitic slates from Uruguay: Petrophysical and petromechanical characterization and deposit evaluation. *Environ. Earth Sci.* **2013**, *69*, 1361–1395. [[CrossRef](#)]
16. Franke, W.; Paul, J. Pelagic redbeds in the Devonian of Germany—Deposition and diagenesis. *Sediment. Geol.* **1980**, *25*, 231–256. [[CrossRef](#)]
17. Cárdenes, V.; Prieto, B.; Sanmartín, P.; Ferrer, P.; Rubio, A.; Monterroso, C. Influence of chemical-mineralogical composition on the color and brightness of Iberian roofing slates. *J. Mater. Civ. Eng.* **2012**, *24*, 460–467. [[CrossRef](#)]
18. Dale, T.N.; Eckel, E.C.; Hillebrand, W.F.; Coons, A.T. *Slate Deposits and Slate Industry of the United States*; Bulletin 275, Series A, Economic Geology; U.S. Geological Survey: Reston, VA, USA, 1906; Volume 63, pp. 1–154.
19. Grossi, J.H.; Chiodi, C.; Kistemann, D. *Panorama do Setor de Ardósias do Estado de Minas Gerais*; Textos e Anexos; Governo de Minas Gerais: Belo Horizonte, Brasil, 1998; Volume 1, pp. 1–90.
20. Krosse, S.; Schreyer, W. Comparative geochemistry of coticles (spessartinequartzites) and their redschist country rocks in the Ordovician of the Ardennes Mountains, Belgium. *Chem. Erde* **1993**, *53*, 1–20.
21. Ministerio de Industria y Energia. *Pizarras de Espana*; Instituto Geologico y Minero de Espana: Madrid, Spain, 1977; p. 83.
22. Zimmerle, W.; Stribny, B. Organic carbon-rich pelitic sediments in the Federal Republic of Germany. *Cour. Forsch. Inst. Senckenberg* **1992**, *152*, 1–144.
23. Jung, D. Mineralogisch-petrographische Untersuchung eines Schiefers aus Bhutan. Unpublished. 2001; 13.
24. Stribny, B.; Urban, H. Classification of sedimentary rocks—Black shale series based on their normative minerals compositions. *IGCP Proj. Newsl.* **1989**, *254*, 30.
25. Jung, D.; Geisler-Wierwille, T. Program “SlateNorm” Version 1.1. Unpublished. 1999–2000.
26. Cardenes, V.; Rubio Ordóñez, A.; Lopez Munguira, A.; Monterroso, C. Petrografía y mineralogía de las pizarras para cubiertas de la Península Ibérica en relación con su calidad. *Trab. Geol. Univ. Oviedo* **2010**, *30*, 412–420.
27. Ferreiro Mählmann, R.; Bozkaya, Ö.; Potel SLe Bayon, R.; Šegvic, B.; Nieto, F. The pioneer work of Bernard Kübler and Martin Frey in very low-grade metamorphic terranes: Paleo-geothermal potential of variation in Kübler-Index/organic matter reflectance correlations. A review. *Swiss J. Geosci.* **2012**, *105*, 121–152. [[CrossRef](#)]

28. Bushan, A. Dachschieferorkommen Deutschlands-petrographisch-geochemische Charakterisierung mit besonderem Blick auf die Goslarer Dachschiefer. Masterarbeit Universität Potsdam. Unpublished. 2017; 1–112.
29. Chemical Formulas of the Minerals with Changes after. Available online: <http://webmineral.com> (accessed on 21 February 2020).
30. Molar Mass Calculator. Available online: <http://www.chemurope.com/en/tools/> (accessed on 21 February 2020).



© 2020 by the authors. Licensee MDPI, Basel, Switzerland. This article is an open access article distributed under the terms and conditions of the Creative Commons Attribution (CC BY) license (<http://creativecommons.org/licenses/by/4.0/>).